Electrochemical and Solid-State Letters, **11** (11) A198-A201 (2008)
1099-0062/2008/11(11)/A198/4/$23.00 © The Electrochemical Society

Cobalt Oxide Nanoparticles Prepared from Reverse Micelles as High-Capacity Electrode Materials for Li-Ion Cells

C. Vidal-Abarca, P. Lavela, and J. L. Tirado*,z

Laboratorio de Química Inorgánica, Universidad de Córdoba, Edificio Marie Curie, Campus de Rabanales, 14071 Córdoba, Spain

A reverse-micelles procedure followed by annealing is developed to prepare Co_3O_4 materials with controlled particle size and microstructure. The single-phase products occur as submicrometric particles that interconnect into larger aggregates with spherical shape and no porosity. Two types of electrochemical response are found in lithium cells depending on annealing time and temperature. Reversible capacities of up to ca. 800 mAh g^{-1} are observed in intermediate annealing, while lower capacities and better capacity retention are found for short treatments at 600°C. These differences are related to the changes in charge-transfer resistance.
 [DOI: 10.1149/1.2975140]

Manuscript submitted June 3, 2008; revised manuscript received July 29, 2008. Published September 2, 2008.

In recent years, new chemical synthesis procedures have been developed for obtaining materials with decreasing particle size. Use of the emerging preparative routes has spread rapidly to a wide variety of industrial applications.[1] Chemical reactions can be confined inside the droplet volume of emulsions stabilized by the formation of micelles. In this way, growth of solid product particles is restricted to micro-nanometric volumes. In addition, surfactant molecules coat the newly formed ultrafine particles, thus avoiding undesirable agglomeration processes. This method has been successfully applied to the preparation of submicrometric oxides and oxysalts.[2]

A noteworthy example of the ability of long-chain organic molecules to impede particle aggregation during the synthesis of monodisperse nanocrystals was developed by Park et al.[3] They found that the decomposition of oleate complexes of transition metals at 320°C allowed the large-scale preparation of metal oxide nanoparticles.

The reversibility of some conversion reactions with lithium involving transition metal oxides, which lead to electrochemical reduction to a metallic state of the transition element, has been recently emphasized.[4] Conversion reactions progress from the surface of the particle of metallic compound inward. For this reason, it is expected that the morphological and textural properties have a direct influence on yields of electrochemical electrode material.

In this article, we describe the use of organic anionic surfactants that stabilize reverse (water-in-oil) micelles containing transition metal water-soluble salts. The particles obtained by reactions of the reverse micelles at room temperature are evaluated as active electrode materials for advanced lithium-ion batteries.

Experimental

A reverse-micelles procedure was used in this study, using Span 80 (sorbitan monooleate, i.e., sorbitan mono-9-octadecenoate, $C_{18}H_{34}O_2$) as the surfactant. The reaction took place by the coalescence of two different reverse micelles containing 1 M aqueous solutions of NaOH and cobalt chloride, respectively. The oil phases selected for this procedure were alternatively hexane and octadecene. Figure 1 shows a schematic representation of the procedure. The resulting pink precipitate product, $Co(OH)_2$, was separated by ultracentrifugation, dried, and annealed for 15 or 24 h under air atmosphere at 600, 800, and 1000°C.

X-ray diffraction (XRD) patterns were recorded in a Siemens D5000 diffractometer, with Cu Kα radiation and a graphite monochromator. A step scan procedure was set with a pass of 0.02° (2θ) and a measuring time of 12 s. Scanning electron microscopy (SEM) images were obtained with a JEOL-SM6300 microscope. Battery tests were carried out by using two- and three-electrode Swagelok-type cells. Counter electrodes were 9 mm disks of lithium metal, and the working electrode consisted of a mixture of 75% active material and 10% graphite, 10% carbon black, and 5% poly (vinylidene fluoride) binder coated on a copper foil of the same diameter. A 1 M $LiPF_6$ [ethylene carbonate/diethyl carbonate = 1:1] electrolyte solution was supported in Whatman glass fiber disks. Galvanostatic tests were carried out on an Arbin galvanostat multichannel system. The imposed kinetic rate was fixed at 1 C for both charging and discharging. Step potential electrochemical spectroscopy was monitored on a MacPile System. Electrochemical impedance spectroscopy (EIS) was carried out in an Autolab PGSTAT12 system. A three-electrode lithium cell was successively cycled by passing current between the working electrode (evaluating material) and the counter electrode (Li). After a period of relaxation, at least 5 h, to achieve a quasi-equilibrium system, the impedance spectra were recorded vs a Li reference electrode. An ac voltage signal of 5 mV was applied from 100 to 2 mHz.

Results and Discussion

The XRD data of samples prepared in water-in-hexane emulsions annealed at different temperatures are shown in Fig. 2a. The product of water-in-octadecene micelles annealed at 800°C for two different periods of time is also shown in Fig. 2. Irrespective of the oil used in the preparation, the patterns can always be indexed in the *Fd*3*m* space group of Co_3O_4 with a normal spinel structure. Thus, the annealing reaction of the solid hydroxide product obtained inside the micellar volume can be written as a topotactical reaction[5]

$$3Co(OH)_2 + 1/2O_2 \rightarrow Co_3O_4 + 3H_2O$$

Upon increasing sintering temperature there is a decrease in line broadening (Fig. 2a) that can be ascribed to a sintering of crystallites. A similar effect is observed after extended annealing at 800°C (Fig. 2b).

Figure 3 shows selected SEM images of different Co_3O_4 samples prepared by the reverse-micelles procedure followed by annealing. Submicrometric particles interconnect with each other, leading to larger aggregates with spherical shape, with no apparent porosity and low surface area as revealed by gas adsorption measurements. Sintering phenomena could be observed by both increasing the an-

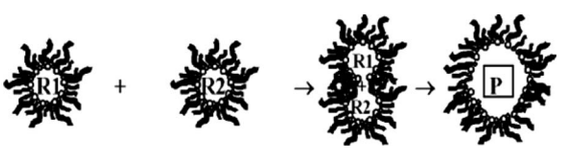

Figure 1. Schematic representation of the reverse-micelles synthetic route used in this study. R1: 1 M aqueous $CoCl_2$; R2: 1 M aqueous NaOH; P: $Co(OH)_2$.

* Electrochemical Society Active Member.
z E-mail: iq1ticoj@uco.es

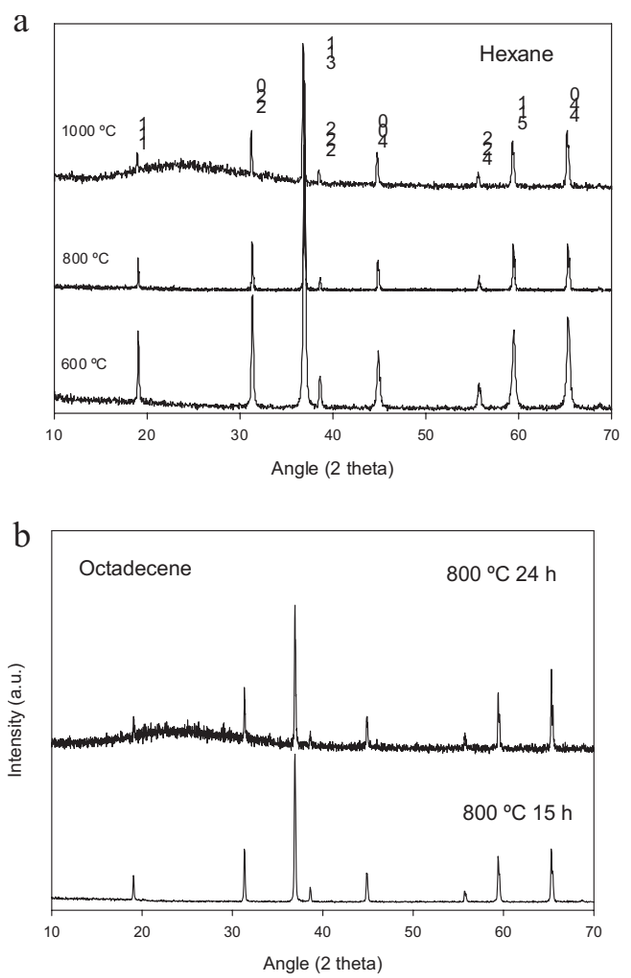

Figure 2. XRD patterns of Co_3O_4 samples prepared in (a) hexane and (b) octadecene and annealed under different conditions.

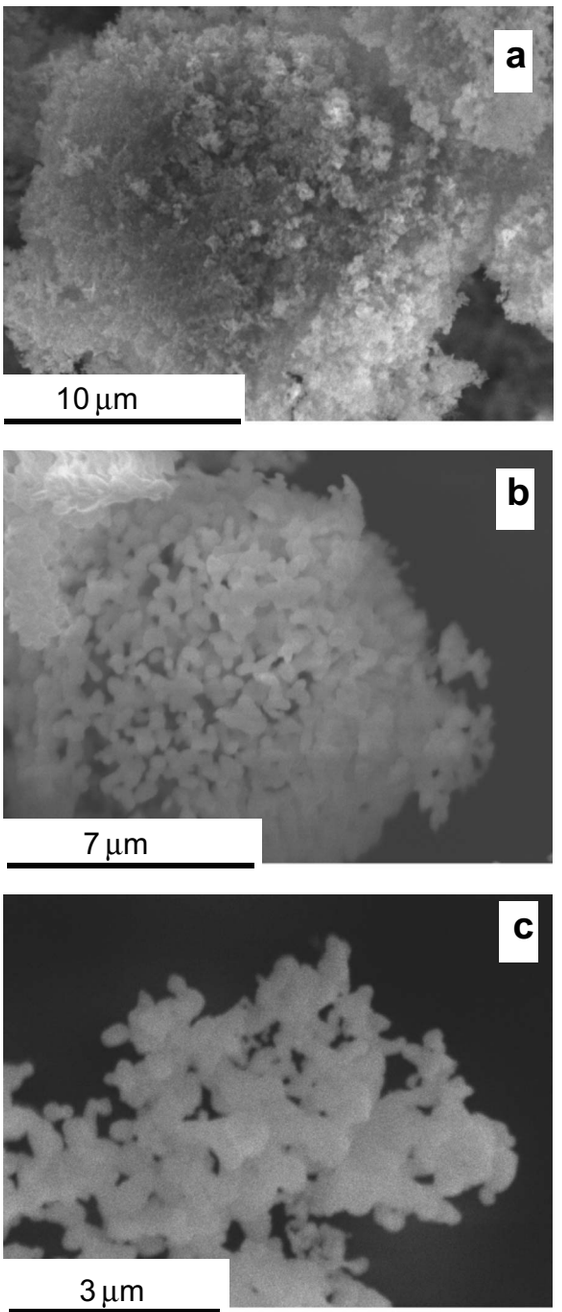

Figure 3. SEM images of Co_3O_4 prepared in hexane and annealed at (a) 600°C for 24 h, (b) 800°C for 15 h, and (c) 800°C for 24 h.

nealing temperature and extending the annealing period. A particularly enhanced increase in the size of the primary particles was observed for samples obtained from emulsions in octadecene annealed at 800°C for periods increasing from 15 to 24 h (Fig. 3b and c). The size of the pores defined within the secondary particles also increased upon increasing size of the primary particles. Consequently, the size of the secondary particles suffered little change with annealing. These results are particularly interesting with a view of tailoring particle size together with particle aggregation to obtain the best materials for each particular application.

The different Co_3O_4 samples were used as the active material in composite electrodes vs lithium metal. The resulting test cells were cycled galvanostatically. Figure 4 shows the charge and discharge branches of the first few cycles of a typical cycling behavior of these samples. Few differences were observed between samples, except for the capacity retention, which is discussed below. The first discharge shows an extension equivalent to reducing the metal ions to the metallic state. The decline in voltage at the end of the discharge is probably related to the formation of a reversible coating with organic side products, as suggested elsewhere.[6] The void space between primary particles in the aggregates ensures access of the electrolyte to the whole mass of active material. The successive charge–discharge cycles display a different profile as a result of the drastic microstructural changes occurring in the first cycle which generates new energy-differing sites.

Figure 5 shows the capacity retention curves. In samples obtained from reverse micelles in hexane and octadecene media and annealed at 600°C for 24 h and 800°C for 15 h, respectively, reversible capacities higher than 800 mAh g^{-1} were obtained for around 20 cycles. Then a decline is observed that could be ascribed to both the positive and the lithium electrode degradation. The similarity between these two samples seems to be related with the previously described effect of annealing time and temperature on particle and pore sizes. An opposite behavior was found for samples obtained at 600°C for 15 h and 800°C for 24 h. Thus, the second discharge capacity is close to 800 mAh g^{-1}, but this value starts a steep decrease immediately afterward and then stabilizes at around 500 mAh g^{-1} until cycle 80. Consequently, the end capacity values are lower for samples annealed at 600°C for 24 h and 800°C for

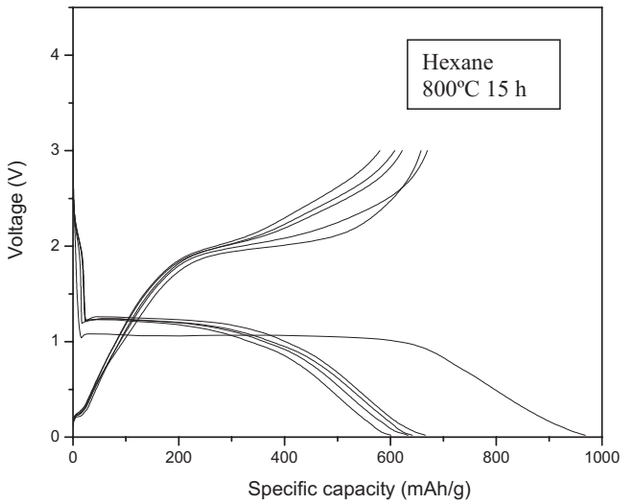

Figure 4. Typical galvanostatic charge/discharge curves for the first few cycles for Co_3O_4 obtained from reverse micelles.

15 h. It can be suggested that the stability of both electrodes increases for low-capacity cycling conditions. The ultrafine primary particles in the solids prepared after short annealing periods at 600°C lead to a rapid deterioration of the electrode surface, but once the electrode stabilizes, the coating effect of the side products could be responsible for the enhanced capacity retention. On the contrary, those samples prepared by long annealing periods at 800°C and, even more notably, at 1000°C (Fig. 5), showed poorer performance, with capacity values always below those previously described, due to the poorer contact with the electrolyte which leads to unused regions of the cobalt oxide particles and consequently, lower capacities.

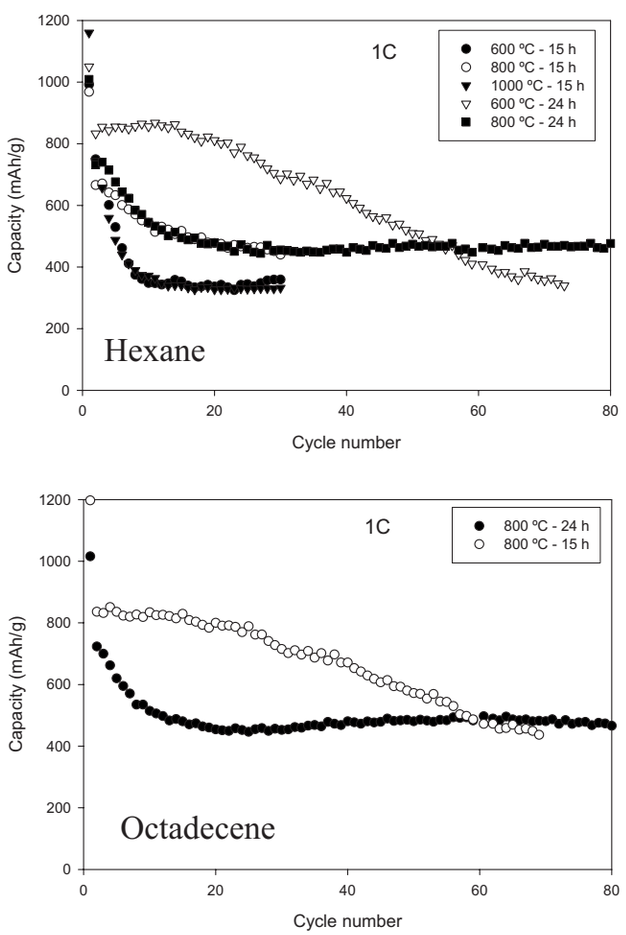

Figure 5. Capacity vs cycle number for lithium cells using Co_3O_4 samples obtained under different conditions.

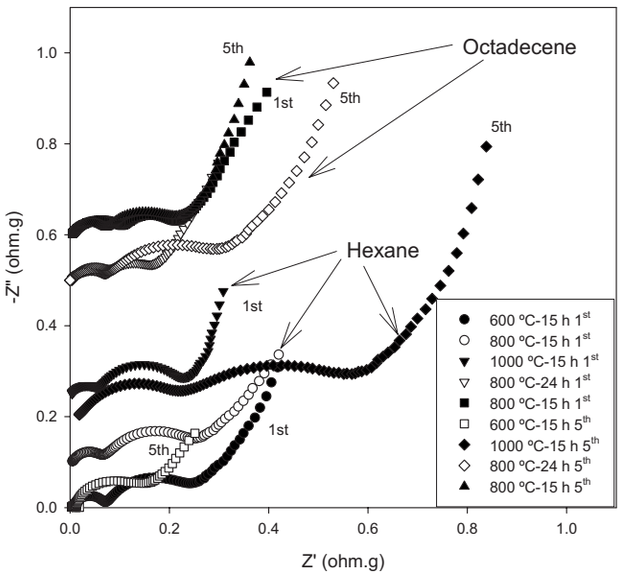

Figure 6. Impedance spectra of electrodes discharged after the first and fifth discharges.

To gain further insight on the differences in capacity retention, surface phenomena were taken into account and EIS data were recorded. Figure 6 displays some Nyquist plots obtained for Co_3O_4 samples. The three-electrode test cells were monitored at the end of the first and fifth discharges. Two depressed semicircles appear at high and intermediate frequencies. These semicircles are respectively assigned to lithium migration through the electrolyte-inorganic solid electrolyte interphase (SEI) film (with R_{sf} resistance and C_{sf} capacity) and charge transfer through the particle surface (R_{ct} and C_{ct}). At low frequencies, a large semicircle scarcely visible can be ascribed to a pseudocapacitance behavior, most probably due to the growth of the polymeric organic layer.[6] The resistance values ascribed to these processes, which are collected in Table I, show that R_{ct} values were commonly higher than R_{sf} values, indicating that the lithium migration through the metallic particle surface imposes a higher energy barrier than the transport through the Li_2O matrix.[7] However, the influence of charge-transfer limitations at the Li electrode on the polarization of the electrochemical curves cannot be discarded as described in Ref. 8.

After the first discharge, R_{sf} values were rather homogeneous, irrespective of the organic solvent used in the synthesis or the annealing temperature. This is basically a consequence of the same chemical nature (Co_3O_4) of the surfaces in which the SEI has to be formed on discharge. From the first to the fifth cycle, there is an increase in R_{ct} resistance, especially for those Co_3O_4 samples having a marked capacity fading during the first cycles. Otherwise, those samples whose capacity values were more affected upon prolonged cycling were also the samples involved in a more notorious increase of charge-transfer resistance with cycling. Moreover, the effect of the annealing temperature is clearly evidenced by R_{ct} resistance values after five cycles for the sample annealed at 1000°C. This behav-

Table I. Values of SEI and charge-transfer resistances for different Co_3O_4 samples. Electrodes were measured at full discharge.

		R_{sf} (Ω g)		R_{ct} (Ω g)	
		1st discharge	5th discharge	1st discharge	5th discharge
Hexane	600°C–15 h	0.071		0.161	
	800°C–15 h	0.081		0.196	
	1000°C–15 h	0.058	0.074	0.164	0.208
Octadecene	800°C–15 h	0.113	0.075	0.087	0.132
	800°C–24 h	0.073	0.08	0.086	0.216

ior can be correlated with the poor electrochemical performance of this sample as compared to other samples prepared at 800°C for different periods of time.

Conclusions

The synthesis method using reverse micelles followed by controlled thermal treatments has allowed cobalt oxide with a spinel structure with tailored size of the primary particles and pore volume to be obtained. The galvanostatic cycles reveal reversible capacities greater than 800 mAh g^{-1} for the particular texture generated by annealing at 800°C for 15 h or 600°C for 24 h. The surface properties of these particular materials affect the impedance of charge transfer and solid electrolyte interface, the first parameter being of prime importance in the capacity retention behavior.

Acknowledgments

We appreciate financial support from the European Commission (contract SES6-CT2003-503532, Alistore), Ministerio de Educación y Ciencia (contract MAT2005-00374), and Junta de Andalucía (contract FQM1447).

Universidad de Córdoba assisted in meeting the publication costs of this article.

References

1. *Springer Handbook of Nanotechnology*, B. Bhushan, Editor, Springer, Germany (2004).
2. M. J. Aragón, C. Pérez-Vicente, and J. L. Tirado, *Electrochem. Commun.*, **9**, 1744 (2007).
3. J. Park, K. An, Y. Hwang, J.-G. Park, H.-J. Noh, J.-Y. Kim, J.-H. Park, N.-M. Hwanh, and T. Hyeon, *Nat. Mater.*, **3**, 891 (2004).
4. P. Poizot, S. Laruelle, S. Grugeon, L. Dupont, and J. M. Tarascon, *Nature (London)*, **407**, 496 (2000).
5. M. Figlarz, J. Guenot, and F. Fievet-Vincent, *J. Mater. Sci.*, **11**, 2267 (1976).
6. S. Laruelle, S. Grugeon, P. Poizot, M. Dollé, L. Dupont, and J.-M. Tarascon, *J. Electrochem. Soc.*, **149**, A627 (2002).
7. P. Lavela and J. L. Tirado, *J. Power Sources*, **172**, 379 (2007).
8. M. Dollé, Ph. Poizot, L. Dupont, and J.-M. Tarascon, *Electrochem. Solid-State Lett.*, **5**, A18 (2002).